Journal of Ceramic Processing Research. Vol. 21, No. 2, pp. 131~142 (2020)
(Received 12 July 2019, Received in revised form 20 January 2020, Accepted 21 January 2020)
https://doi.org/10.36410/jcpr.2020.21.2.131

J O U R N A L O F
Ceramic Processing Research

Multi objective optimization of wear characteristics on Al 7075/Al_2O_3/B_4C composites - Desirability approach

Pridhar. T[a,*], Ravikumar. K[b], Sureshbabu. B[a], Srinivasan. R[a] and Sathishkumar. B[a]
[a]*Department of Mechanical Engineering, Sri Krishna College of Technology, Coimbatore, India*
[b]*Department of Mechanical Engineering, Dr.NGP Institute of Technology, Coimbatore, India*

Aluminium hybrid metal matrix composites comprises of Al alloy embedded with multiple hard particulates to improve the wear characteristics. In this study Al 7075/Al_2O_3/B_4C hybrid composite was fabricated with 5 wt.% B_4C particles addition and 2, 4, 6, 8 and 10 wt.% of Al_2O_3 by liquid metallurgy route. The dry sliding wear behaviour of hybrid composites was investigated under various sliding parameters using a pin on disc tribometer. Numerical models were developed to predict the frictional and wear characteristics of the composites. Analysis of variance method and confirmation experiments were employed to validate the adequacy of the developed model. The composites with high particle content exhibits better wear resistance at various sliding conditions. Detailed metallurgical investigations were carried out on the on worn surface. The wear rate was severe at higher loads due to the crater formation and in addition to abrasive wear. The wear rate and coefficient of friction were optimized using desirability based multi criteria optimization technique.

Keywords: Alumina, Boron carbide, SEM, XRD, EDS, Dry sliding wear, RSM, Optimization.

Introduction

Composite materials have become a need in the modern decade to obtain numerous properties which were not achieved by monolithic materials. It caters the increasing demand for enhanced mechanical and tribological properties in aerospace, marine, defence and automotive applications [1-3, 40]. The commonly used techniques in fabrication of hybrid metal matrix composites (HMMC) are stir casting and powder metallurgy technique. Stir casting route has remained as the most explored technique for fabrication of hybrid composites due to its flexibility, simplicity and commercial viability [4, 5, 38, 39]. Baradeswaran et al. [6] observed that the addition of aluminium oxide to base alloy improved the tensile strength, hardness, flexural strength and compression strength. Also the inclusion of graphite improved the wear characteristics of the hybrid composites. Investigations of Veeresh Kumar et al. [7] on addition of silicon carbide and aluminium oxide to aluminium alloy indicate improvement in density, tensile, micro hardness and wear of the base alloy. Ravikumar et al. [8] observed that the wear in Aluminium/flyash composites, decreased with increased fly ash particle size primarily due to the interfacial strength between the base metal and its reinforcement. Dora Siva Prasad et al. [9] in the studies of tribological behavior on A356/SiC/Rice Hush Ash (RHA) composites observed that increase in wear resistance was owing to the strengthening mechanism of the matrix due to the thermal mismatch between the reinforcements and the base alloy. Ravinder Kumar et al. [10] made an investigation on Al 7075/SiC/graphite and concluded that load was the most noteworthy factor that affects the wear rate. On observation of the wear SEM image of Al/SiC/mica composites Rajmohan et al. [11] reported that numerous long grooves and craters were found on worn surfaces at higher load and the mechanism changed from abrasive wear to delamination at higher load. Uthayakumar et al. [12] observed high melt wear at high sliding speed and higher load because of the higher order existence of local stress. Krishnan et al. [13] revealed that abrasive wear prevails in particle reinforced composites, whereas adhesive wear was dominant in base alloy. Radhika et al. [14] found a MML layer in the surface which formed due to the increase in velocity on the counter face of the specimen. An attempt has been made by Ravikumar et al. [15] to predict the wear rate and coefficient of friction of Al356/fly ash composites using Artificial Neural Network (ANN). Ravinder Kumar et al. [10] made a comparison between Response Surface Methodology (RSM) and ANN for the prediction of Surface roughness measurement on Al 7075 hybrid composites and concluded that prediction of RSM is good as compared to ANN. S. Selvi et al. [16] developed a mathematical model for calculation of wear rate using response surface methodology. Suresh et al. [17] applied RSM Box Behnken design method effectively to reduce the number of trials and to develop a mathematical model with high confidence level and

*Corresponding author:
Tel : +919790003531
E-mail: preeth_t@rediffmail.com

employed ANOVA to verify the adequacy of the mathematical model. Vembu et al. [18] developed a second order polynomial equation for the prediction of tensile strength using RSM. Ravikumar et al. [19] employed a multi response optimization technique based on desirability approach to reveal the optimal process parameters of WEDM on Aluminium hybrid composites. Ravikumar et al. [20] applied desirability based multi response optimization to optimize the wear rate and coefficient of friction in abrasive wear test.

From the above literature survey it is evident that many researchers have put tremendous efforts to manufacture light weight and efficient material for the automobile, marine and aerospace industries. However limited works were carried out on Al 7075 hybrid composites.

Al 7075 aluminium alloy is being used to manufacture rock climbing equipment, automotive components, hang glider airframes, M16 rifles and aerospace applications due to their high strength to weight ratio and good mechanical properties. The present investigation is to manufacture Al 7075 hybrid composite by reinforcing the Al_2O_3 and B_4C particulates and to study the dry sliding wear of the hybrid composites. Scanning electron micrographs (SEM) were used to study the influence of parameters on wear mechanisms. A mathematical model was developed to predict the wear rate and coefficient friction using RSM. The model adequacy was tested using ANOVA. Desirability based Multi response optimization technique was instituted to predict the optimized parameters. The significance of this study is to develop a low weight superior strength material in an affordable cost. This novel material may replace current used alloys with superior quality. The Desirability optimization technique which is used in this research is user friendly and has more accuracy compared to other optimization techniques.

Experimental Procedure

Materials

The composite comprises of Al 7075 as base material, alumina and boron carbide as reinforcement. The chemical composition of the matrix metal (Al 7075) used for the current study is shown Table 1. Al_2O_3 and B_4C particulates are used to manufacture the composite with an average particle size of 40 microns.

The casting was prepared using stir casting machine shown in Fig. 1, Al 7075 reinforced with 2, 4, 6, 8 and 10 wt.% alumina with constant 5 wt.% of boron carbide were prepared by a stir casting technique. A weighed amount of Al 7075 alloy was superheated to 750 °C in a conical shaped graphite crucible by using an electrical resistance furnace. The melt was degassed using solid dry hexachloroethane (C2 Cl6). The particulates were preheated at 700 °C for 20 min. to remove the moisture content and the reinforcements were added to the vortex at a constant feed rate. The composite slurry was stirred continuously at a speed of 530 rpm for 15 minutes. 2 wt% of magnesium was also included to enhance the wettability of the composites.

For proper mixing of the reinforcements with the matrix alloy, stirring was continued for about 10 min even after the completion of particulate additions. For comparative study, unreinforced aluminium alloy was also prepared under similar cast conditions.

Micro Structural Examinations

The microstructure of Al 7075/Al_2O_3/B_4C composites was examined using a scanning electron microscope (JSM-6360). The cast samples for microstructure investigation were polished metallographically. The Polished specimen was then etched with 10% of sodium hydroxide solution and examined for uniformity in distribution of particulates in cast specimens. X-ray Diffraction technique was employed to ensure the presence of base alloy and its dispersed reinforcements.

Fig. 2 represents the SEM micrographs of Al 7075/Al_2O_3/B_4C composites. It is evidently exposed that the dispersion of the particulates are embedded into the Al 7075 aluminium matrix. Further the image reveals the homogeneity of reinforcement in the specimen which indicates the effectiveness of dispersion of the particulates during stirring. XRD of the cast specimen Fig. 3

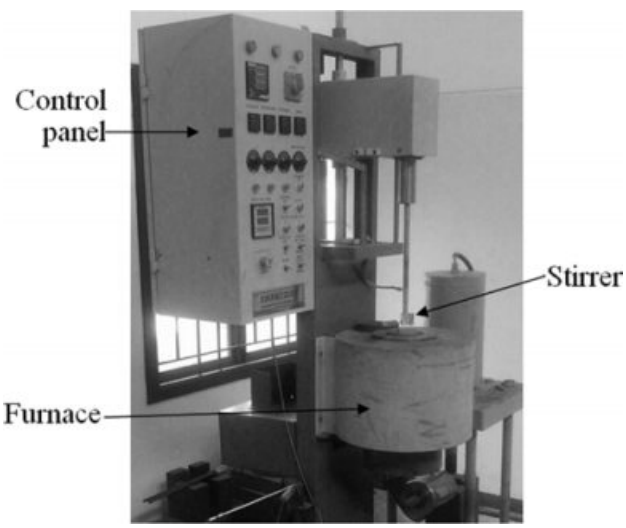

Fig. 1. Stir casting setup.

Table 1. Chemical composition of Al 7075 by Weight percentage.

Chemical Composition	Si	Fe	Cu	Mn	Mg	Cr	Zn	Ti	Al
AL 7075	0.4	0.5	1.6	0.3	2.5	0.15	5.5	0.2	Balance.

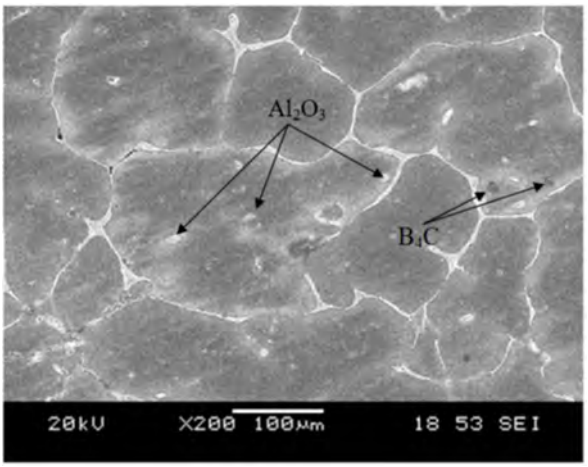

Fig. 2. SEM image of 4% Al_2O_3reinforced hybrid composites.

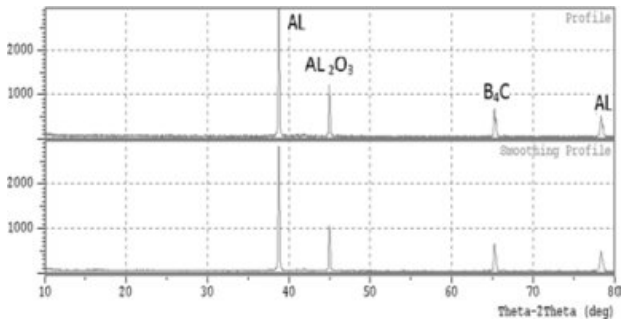

Fig. 3. XRD Analysis of the hybrid composites.

confirms the presence of Al_2O_3 and B_4C particulates in the composites.

Wear Test

Dry sliding wear behaviour of hybrid composite specimens was investigated using Ducom TR 20 pin on disc apparatus as per ASTM G99 standards. The wear testing machine is shown in Fig. 4.

The specimens were machined for 10mm in diameter and 40mm in length and polished with emery paper of grade 600, 800, and 1,000 respectively. The cast pins were then pressed against an EN32 steel disc of surface roughness 1.2 µm and a hardness of 65HRC at room temperature. The frictional forces were documented during the entire wear experiments and average value was recorded. The initial weight of the sample was measured using an electronic weighing machine

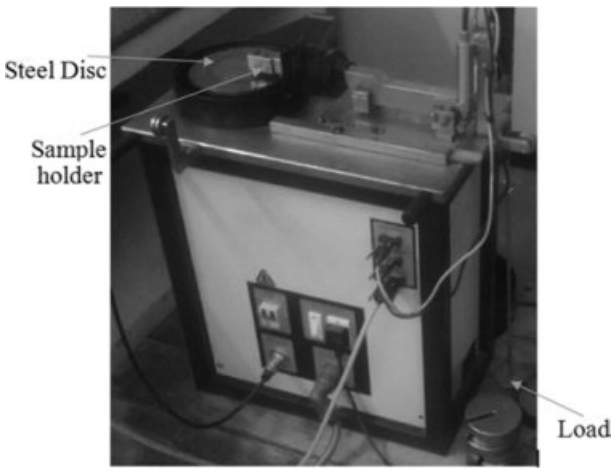

Fig. 4. Ducom TR 20 wear testing machine.

(SHIMADZU BL-220H) with the accuracy of 0.01mg. The pin was weighed before and after testing to find out the amount of weight loss. The wear rate was calculated using the eq. (1) based on the mass loss

$$W = \frac{M}{\rho D} \tag{1}$$

where W is the wear rate (mm^3/m), M is mass loss (g), ρ is the density (g/mm^3) and D is the sliding distance (m).

The co-efficient of friction was determined by dividing normal force against frictional force. The Dry sliding wear test were conducted as per the design matrix established is shown in Table 2.

Response Surface Methodology and Mathematical Modelling

Response surface methodology

Response Surface methodology is a collection of mathematical and statistical techniques used for empirical model building. It identifies the relations between wear parameters and response functions with minimal number of experiments [21]. Design Expert 10.0 was employed for designing the experiments and to study the influence of parameters on wear rate and coefficient of friction of the hybrid composites. The four factors that affect the wear rate and Coefficient of friction are % reinforcement (R), load (L), sliding distance

Table 2. Sliding wear parameters and their levels.

S.No	Parameters	Designation	Level				
			-2	-1	0	1	2
1	Reinforcement (%)	R	2	4	6	8	10
2	Load(N)	L	10	20	30	40	50
3	Sliding distance(m)	D	250	500	750	1000	1250
4	Speed(m/s)	S	0.4	0.8	1.2	1.6	2.0

(D) and speed (S). A central composite design (CCD) model was chosen to determine the dry sliding wear behaviour of the cast composites. The levels of each factor were chosen as 2, -1, 0, 1 and 2 in the coded form. The sliding wear parameters and their levels are given in Table 2. The trials were carried out as per the design matrix and their responses are presented in Table 3.

Development of mathematical model

A second order polynomial regression model is constructed to predict the relationship between the parameters and their responses which shown in eq. (2).

$$Y_n = c + \sum c_1 x_{iu} + \sum c_{ii} x_{iu}^2 + \sum c_{ij} x_{iu} x_{ju} \quad (2)$$

where Y is response c, c_i, c_{ii} and c_{ij} are coefficient respectively.

The response function representing the wear parameters, namely, percentage as a function of reinforcement (R), load (L), sliding speed (S) and sliding distance (D) can be expressed as Y = f(R, L, S, D), where Y is the response. A numerical model was developed using Design Expert Software R10 and the regression coefficients are calculated. The non-significance coefficients were curtailed and the mathematical models developed for predicting the wear rate and coefficients of friction in coded form are given in eq. (3) and eq. (4).

$$\text{Wear rate (W)} \times 10^{-3}\ \text{mm}^3/\text{m} = 1.6501 - 0.4487(\text{R}) + 0.1556(\text{L}) - 0.1119(\text{D}) - 0.13715(\text{S}) + 0.0329(\text{RD}) \quad (3)$$

$$\text{Coefficient of friction (F)} = 0.3266 - 0.0107(\text{R}) + 0.0047(\text{L}) + 0.0004(\text{D}) - 0.0129(\text{S}) + 0.0035(\text{D})(\text{S}) - 0.0013(\text{L}^2) \quad (4)$$

Development of mathematical model

Normality of data

Normality of data is investigated by plotting a graph between the residuals and the normal probability [22]. The probability plot for wear rate and coefficient of friction is shown in Fig. 5. From the plot it is evident that the residuals fall on a straight line and the errors

Table 3. The coded design factors and responses.

Ex. no	Run Order	% of Al_2O_3	Load (N)	Distance (m)	Speed (m/s)	Wear rate ($\times 10^{-3}$ mm^3/m)	Co-efficient of friction
1	26	0	0	0	0	1.7210	0.3240
2	18	2	0	0	0	0.7875	0.3060
3	14	1	-1	1	1	0.8860	0.3024
4	19	0	-2	0	0	1.2456	0.3085
5	2	1	-1	-1	-1	1.2922	0.3312
6	15	-1	1	1	1	1.9272	0.3353
7	11	-1	1	-1	1	2.3000	0.3220
8	24	0	0	0	2	1.2930	0.2984
9	23	0	0	0	-2	1.9200	0.3601
10	4	1	1	-1	-1	1.5770	0.3342
11	29	0	0	0	0	1.7250	0.324
12	31	0	0	0	0	1.7250	0.3240
13	17	-2	0	0	0	2.4300	0.3562
14	30	0	0	0	0	1.6220	0.3224
15	6	1	-1	1	-1	0.9930	0.3212
16	7	-1	1	1	-1	2.4740	0.3452
17	21	0	0	-2	0	1.9752	0.3214
18	1	-1	-1	-1	-1	2.2400	0.3460
19	16	1	1	1	1	1.2100	0.3144
20	8	1	1	1	-1	1.2840	0.3312
21	12	1	1	-1	1	1.2750	0.3012
22	27	0	0	0	0	1.6120	0.3340
23	10	1	-1	-1	1	1.0200	0.2943
24	5	-1	-1	1	-1	1.9850	0.3420
25	20	0	2	0	0	1.8920	0.3392
26	22	0	0	2	0	1.4223	0.3220
27	25	0	0	0	0	1.6120	0.3242
28	9	-1	-1	-1	1	1.9123	0.3231
29	28	0	0	0	0	1.6120	0.3342
30	3	-1	1	-1	-1	2.4530	0.3515
31	13	-1	-1	1	1	1.7300	0.3219

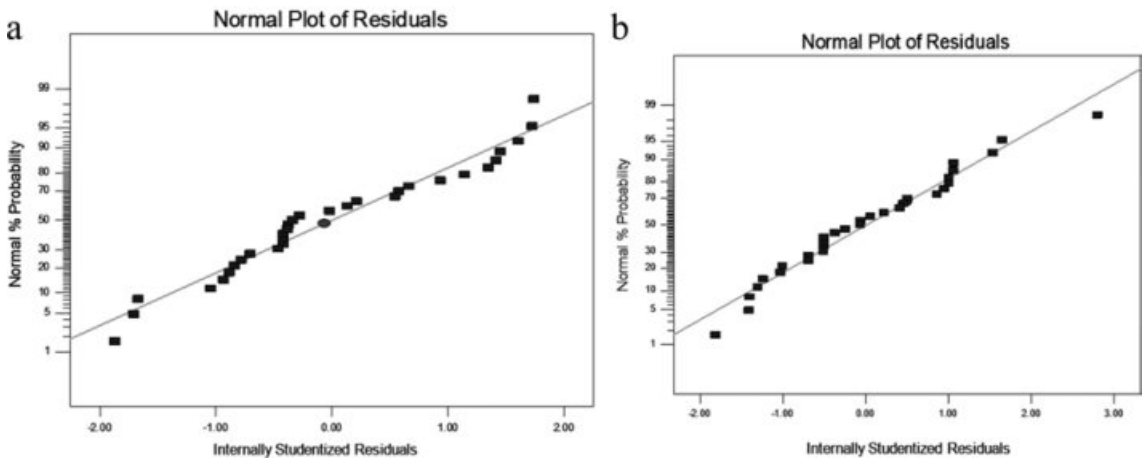

Fig. 5. Normal probability plot (a) wear rate (b) coefficient of friction.

are distributed in normal showing accuracy of the model.

Independency of the data

Independency of the data was tested by means of residual plot. This was done by plotting the residuals against run order [23]. Fig. 6, shows the residual plot for wear rate and coefficient of friction respectively. This plot depict that the no predictable pattern was observed because almost all the residuals lies between -2 to 2 levels.

Analysis of variance

Adequacy of the developed model was checked using ANOVA technique. The correlation coefficient (R^2) indicates the goodness of fits for the model [13]. In this work, the value of regression coefficient ($R^2 = 0.9774$) and adjusted regression coefficient (adjusted $R^2 = 0.9728$) indicates that only 5% of the total variations are not explained by the model. The value of "Prob < F", which depicts that the model is statistically significant [24].

The ANOVA test results of wear rate were presented in Table 4. The square of the regression coefficient (R^2) value 0.9774 confirms that equation 3 is highly reliable. In addition the computed F value = 174.72 is greater than the tabulated value F (5, 25) = 3.85, suggesting that the test is more accurate. The P value (< 0.0001) indicates that the empirical model is statistically significantly [25].

The ANOVA test results of coefficient of friction were depicted in Table 5, the Square of the regression coefficient R^2 value 0.9239 confirms that equation (4&5) is highly reliable. In addition, the computed F value 60.68 is more than the tabulated value F (5, 25) = 3.85, confirming that the test is significant. The P value (< 0.0001) admits that the empirical model is significant. Thus the proposed mathematical model

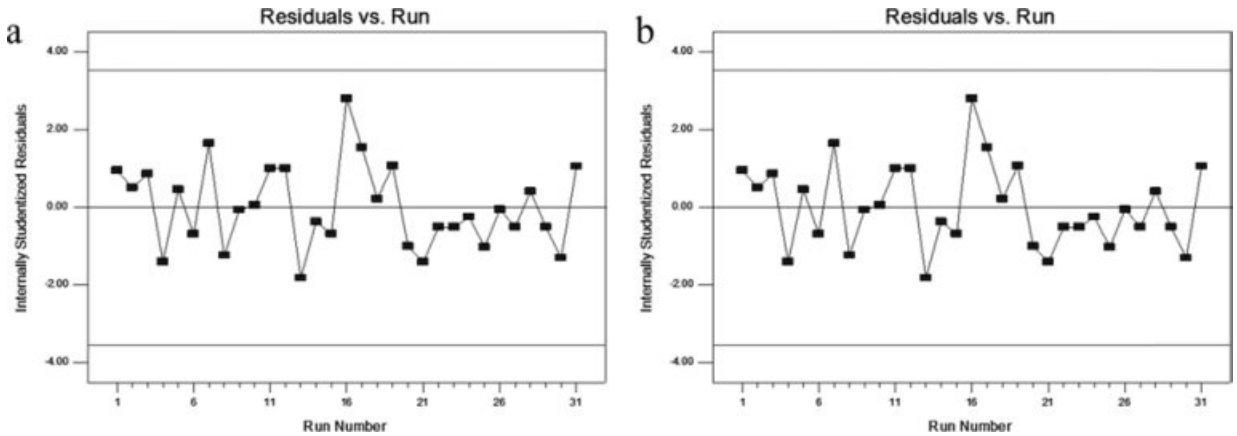

Fig. 6. Residual plot (a) wear rate (b) coefficient of friction.

Table 4. ANOVA results of wear rate using the mathematical model.

Source	Degrees of freedom	Sum of square	Mean of square	F-Value	P-value
Model	6	6.183E-006	1.237E-006	Fcal = 174.72 Ftab=3.85	< 0.0001 suggested
Residual	24	1.432E-007	5.728E-009		
Lack of fit	18	1.227E-007	6.457E-009		
Pure error	6	2.052E-008	3.419E-009		
Corr.Total	30				

$R^{2:}$ 0.9774 adjusted R^2: 0.9728 and predicted R^2: 0.9631

Table 5. ANOVA results of coefficient of friction using the mathematical model.

Source	Degrees of freedom	Sum of square	Mean of square	F-Value	P-value
Model	5	7.544E-003	1.509E-003	Fcal = 60.68 Ftab=3.85	< 0.0001 suggested
Residual	25	6.216E-004	2.486E-005		
Lack of fit	19	4.654E-004	2.450E-005		
Pure error	6	1.562E-004	2.603E-005		
Corr.Total	30				

R^2: 0.9239 adjusted R^2: 0.9086 and predicted R^2: 0.8839

could be used for the prediction of coefficient of friction of the hybrid composites

Results and Discussion

Study of Wear Behaviour of Al 7075/ Al_2O_3/B_4C hybrid composites

Fig. 7 & 8, represents the 3D interaction effect of the input parameters on wear rate and coefficient of friction on aluminium hybrid composites. From the equation (3 & 4), it can be ascertained that the wear rate and coefficient of friction were fundamentally influenced by reinforcement percentage and preceded by load, distance and speed.

Effect of parameters on wear rate

The influence of input parameters on wear rate is represented in Fig. 7. The effect of reinforcements and load on wear rate was depicted in Fig. 7(b). The inclusion of reinforced particulates in Al 7075 alloy decreased the wear rate compared with the base alloy. The wear rate declined due to the reinforcements which act as a load bearing ingredients thereby restricting the material removal in composites. Fig. 7(b), depicts a 2D contour plot, with different colour, namely blue for minimum value, cyan for medium value, green for high and red for very high value. The plot indicates that wear rate increases with increase in load at minimum reinforced conditions. A similar trend was observed by [26, 41] in their work on adhesive wear behaviour of metal matrix composites. It is also attributed that increase in reinforcement percentage increases the dislocation density at the time of solidification process resulting in interruption of particle dislocation movement and improving the wear rate of the composites [27].

The wear rate of the base alloy was higher than that of the hybrid composites for all the load conditions. The surface plot depicts that wear rate accelerated with increasing in load. An externally applied load on to the cast samples with continuous contact on the counter face, deforms the surface of the sample, which in turn leads to thermal softening of the specimen and the wear

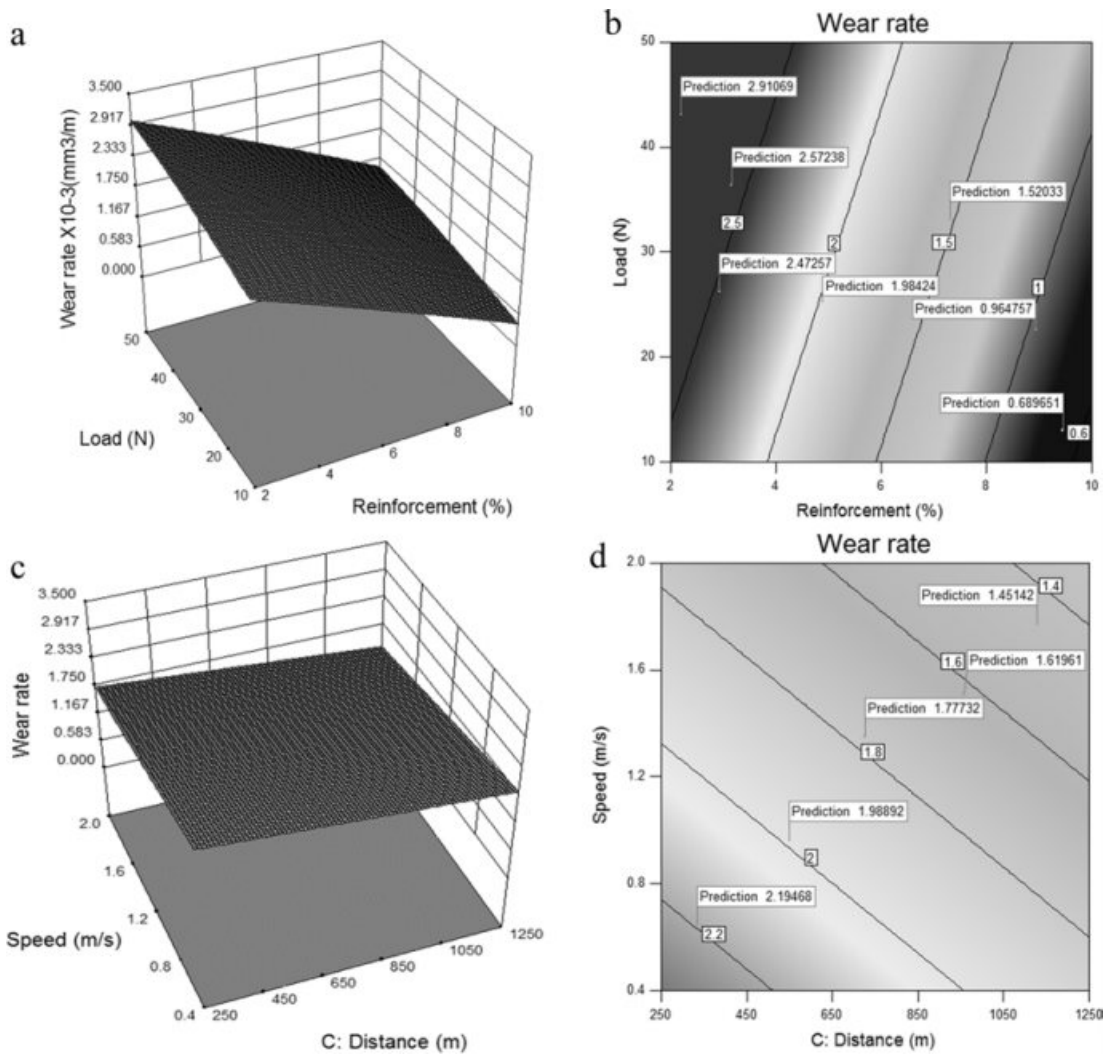

Fig. 7(a-d). Interaction plot for wear rate (a, b) 2D Contour plot (c, d).

regime changes from mild to severe wear. A similar observation was recorded by [6] and [14] in wear study of Aluminium hybrid composites. In summary, the % of reinforcements has negative effect on the wear rate and it accelerates with the applied load.

The influence of speed and distance on the wear rate is represented in Fig. 7(c, d). The 3D surface plot and 2D counter plot indicates that the wear rate declined with increasing speed and sliding distance. When the sliding speed increases, a frictional heat was observed at the contact surfaces and a molten layer was formed which in turn reduces the wear rate. It is also recognized that the reinforcements bear a significant portion of load applied on the composites during the test. At higher speeds the fragmented wear debris particles are forced to combine with the specimen and form a mixed layer, which in turn contribute to the better wear resistance. A similar type of behaviour was observed by [28] & [29]. During increase of sliding distance the hard ceramics available on the surface of the specimen were polished out producing a lower wear rate. Abedini et al. [30] reported that at higher sliding distance oxide layers were formed on the surface which was the main reason for the declination of wear rate in the hybrid composites.

Effect of parameters on coefficient of friction

The influence of input parameters on coefficient of friction is represented in Fig. 8. The effect of reinforcement and load was presented in Fig. 8(a, b). The chart depicts that coefficient of friction decreases with addition of reinforcement. It may be credited due to the addition of alumina and boron carbide to the base alloy where the surface asperities prevent the counter face from mating with the rotating disk. This reduces the coefficient of friction. A related result was revealed by [31] in Al 7075/ SiC /B_4C composites.

The coefficient of friction was increasing with respect to the given load conditions. Initially coefficient of friction increases gradually and it accelerates with the higher load conditions. Singh [32] reported that at initial loads, an oxide layer was formed with low shear strength and ductility which reduces the metal to metal contact. But at higher load conditions the oxide layers

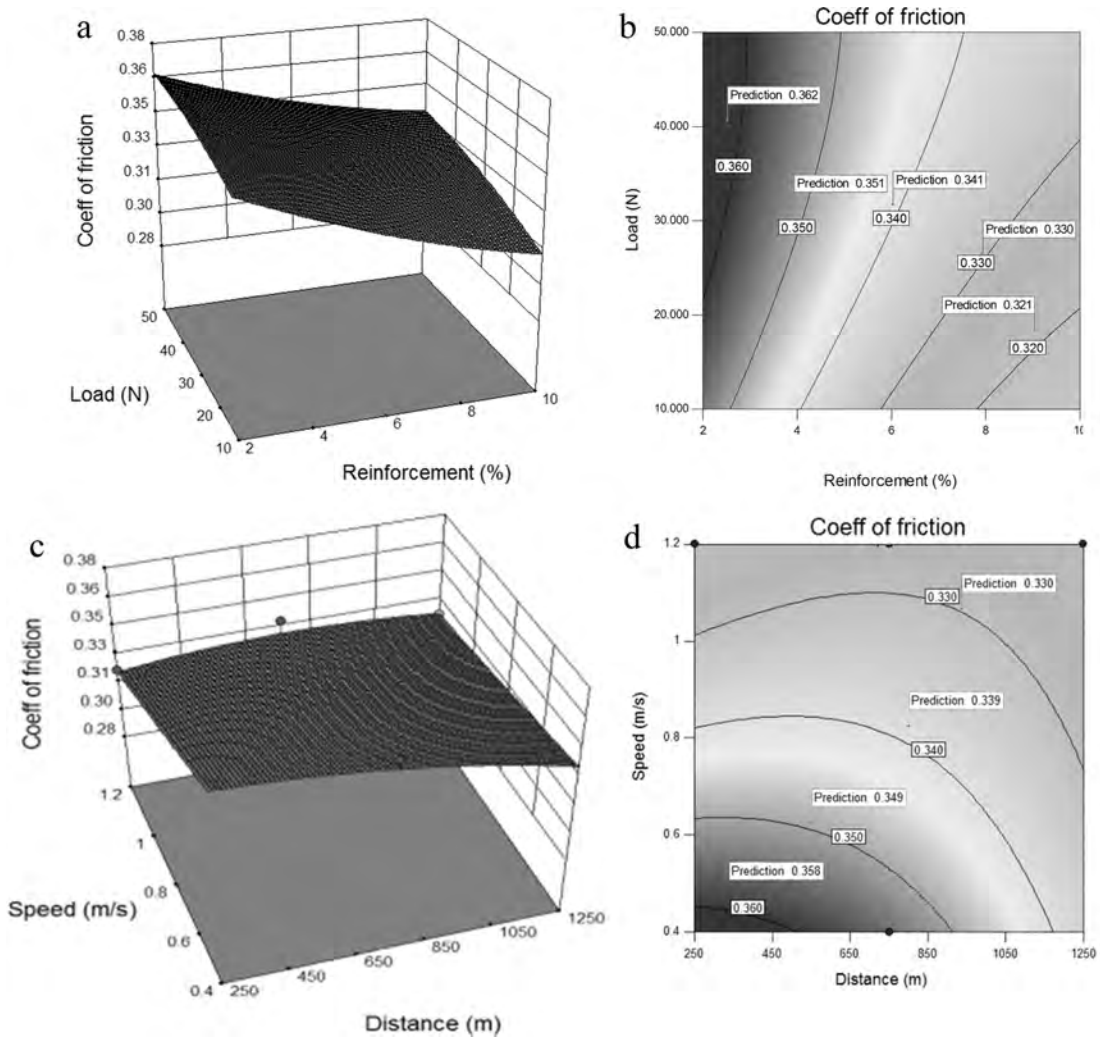

Fig. 8(a-d). Interaction plot for coefficient of friction (a, b) 2D Contour plot (c, d).

were not capable of preventing metal to metal contact resulting in higher coefficient of friction.

The influence of sliding speed and distance on coefficient of friction is represented in Fig. 8(c, d). The 3d plot depicts that increase in sliding speed decreases the coefficient of friction. At higher sliding speed the specimen gets thermally softened due to increase in interfacial temperature, which in turn leads to a lower coefficient of friction. These results were well matched with [33] experimentation in Al/SiC/B_4C Composites. Similarly Hemanth et al. [34] pointed out that higher sliding speed resulted to the lower coefficient of friction. The plot also indicates that increase in sliding distance decreases the coefficient of friction. It may be credited to the presence of Al_2O_3 and B_4C which cater abrasion resistance, resulting in negative effect to the coefficient of friction. These results were well correlated with [35] investigated in A390/G_rp composites, second order polynomial regression model is constructed is investigated by plotting a graph between the residuals and the normal probability. The probability plot for wear rate and coefficient of friction is shown in Fig. 5. From the plot it is evident that the residuals fall on a straight line and the errors are distributed in normal showing accuracy of the model.

Validation

The mathematical models developed by regression analysis were checked for their aqdequency using confirmation experiments. The different input parameters, predicted and actual responses were measured and reported in Table 6. From the results it was evident that percentage of errors between the actual and the predicted values were within the acceptable range. Hence the model is highly efficient in predicting the wear rate and coefficient of friction with 95% confidence level.

SEM Analysis

Scanning Electron Microscope (SEM) studies of the worn specimens were carried out using JOE JSM 6360 make equipment. It can be observed from Fig. 9(a) that the composite with 2% Al_2O_3 was characterized by delamination type of wear due to the adhesion between the composite pin and the disc surface. This is due to the presence of fewer amounts of Al_2O_3 particles in the composite leading to the higher material removal from the surface. Uthayakumar et al. [12] studied the micrograph of Al/SiC/B_4C composites and the results were well agreed with above observations. With an increase in Al_2O_3 it can be observed that the delamination type of wear behaviour was transformed to abrasive type of wear mechanism due the increase in Al_2O_3 and B_4C particle content (Fig. 9(a-f)). The abrasive type of wear mechanism is characterised by plastic deformation whereas the delamination is due to elastic deformation.

Decrease in wear rate is due to the increased bonding strength between the Al_2O_3 and the aluminium matrix defending the composite surface against delamination. The presence of shallow wear grooves running parallel to the direction of loading was established along the surface of the specimen (Fig. 9(b-c)). This is due to the ploughing of the fractured Al_2O_3 particles along the surface in the form of wear debris. With a further increase in Al_2O_3 to 6% (Fig. 9(d-f)) and greater, the presence of both abrasive wear and delamination in the form of patches were observed along the surface. This can be correlated to the ANOVA results that increase in Al_2O_3 and B_4C decreases the wear rate.

Higher wear rate at higher loads was characterised due to the formation of crater in addition to the abrasive wear (Fig. 9(f)). The protrusion of the Al_2O_3 particles is also evidenced in the composite specimen at higher loads (Fig. 9(c)). This confirms the results observed in Fig. 9(d) that an increase in load increases the wear behaviour of the composite. Selvi et al. [16] reported that high abrasive wear occurs at higher loads. The formation of debris in the form of flakes was prime mechanism at higher speeds due to the thermal softening of the material leading to a decrease in wear rate as shown in Fig. 7(c). This may due to the fact that with an increase in sliding speed, the effective indentation due to the Al_2O_3 particles will be reduced due to the entrapment of the debris in the space between the Al_2O_3 present in the composite.

The worn surface of the hybrid composite under 20N load was analysed using energy dispersive spectrometer (EDS). Fig. 10 shows the EDS plot of 4% Al_2O_3 reinforced composite. The presence of Fe indicates the transfer of iron from the counter disc to worn surface of the specimen which results in forming of mechanically mixed layer on the wear surface. Oxygen present in the composite confirms the oxidation reaction, which in

Table 6. Mathematical comparison of actual and predicted results of wear rate and coefficient of friction model.

Process Parameters in coded form				Actual values		Predicted values		% of Error	
Al_2O_3 (%)	Load (N)	Distance (m)	Speed (m/s)	Wear Rate $\times10^{-3}$ (mm^3/m)	Coeff	Wear Rate $\times10^{-3}$ (mm^3/m)	Coeff	Wear	Coeff
1	2	2	1	1.265	0.322	1.2167	0.3151	3.96	2.18
1	1	1	2	1.3569	0.3192	1.2853	0.3011	5.57	6.011
2	1	1	2	0.795	0.30467	0.8366	0.2903	4.97	4.95
-1	0	0	1	1.832	0.3142	1.9616	0.3266	6.61	3.79
				Average				5.27	4.23

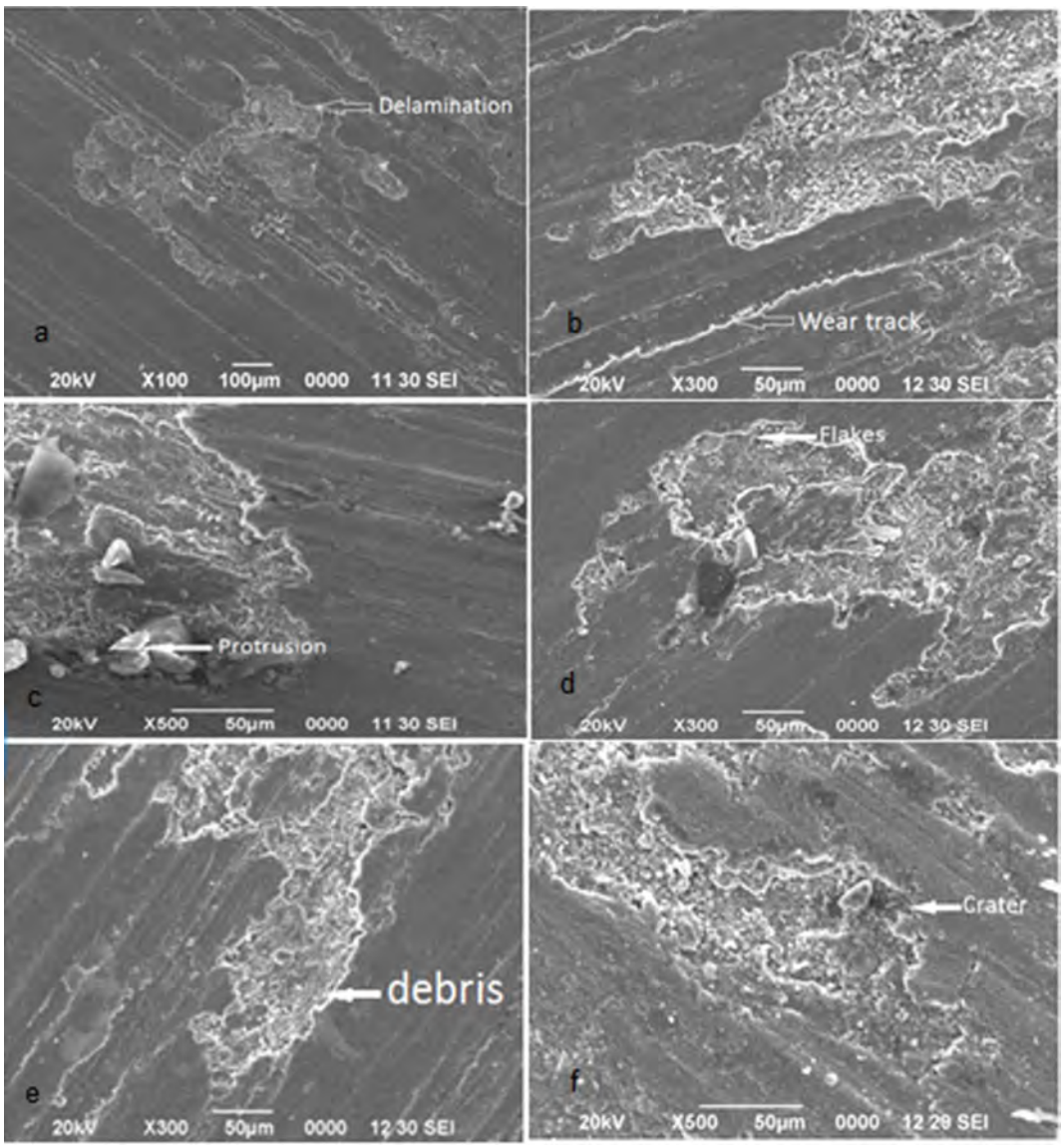

Fig. 9(a-f). Worn Surfaces of Al Hybrid composite specimen under various conditions.

turn reduces the wear rate.

Fig. 11 shows the overlay contour plot wear of Al/Al_2O_3/B_4C hybrid composites in terms of % reinforcement in abscissa and load in ordinate. It is evident from the plot that wear rate of hybrid composites continuously declines with increase in reinforcement % for all load conditions. It is also observed that the wear rate improved with increase in load for any amount of reinforcements. The wear rate increases from 2.136 to 2.390 for an increase in load (X2) from 17.7 to 32.9 for similar % reinforcement (X1). It is credited to the third body abrasion of pull out and protruded particulates which can be observed in Fig. 9(c). The coefficient of friction is reduced with increase in load and % of reinforcement. It may be attributed that the reinforced ceramics prevents the mating between the specimen and the disc, which in turn reduces the coefficient of friction.

Desirability Based Multi Response Optimization

It is a challenging task to select the optimal process parameter combinations for achieving improved wear rate and coefficient friction. Girish et al. [36] employed Taguchi experimental design to optimise the tribological parameters on wear rate. Derringer et al. [37] explained a novel procedure on multiple response optimization named Desirability approach. It is a smart technique used for optimizing the multiple response problems. An objective function is created named desirability function is transformed to an estimated response called desirability, which ranges from 0 to 1. The range respresents from least to the ideal case. Gopalakannan et al. [19] applied combined central composite design and desirability approach to improve the EDM characteristics of aluminium matrix composites. The desirability evaluation was done using Design Expert 10.0 software.

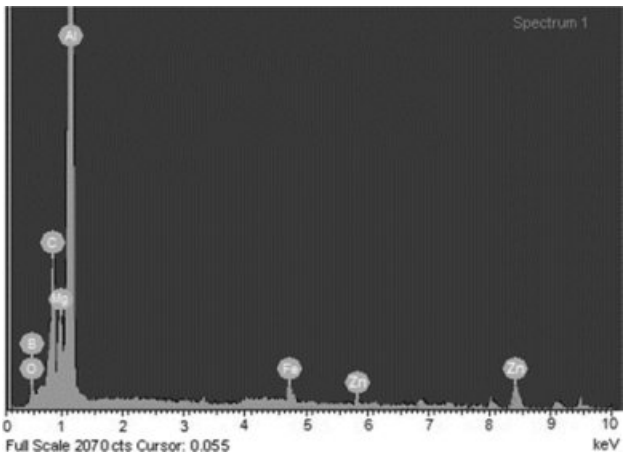

Fig. 10. EDS analysis of worn surface at a load of 20N with 4% Al_2O_3.

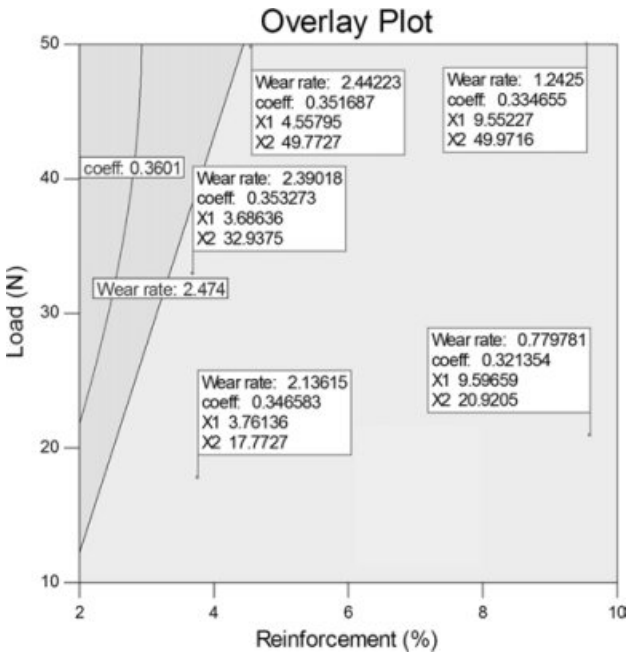

Fig. 11. Over lay counter plot for the effect on wear rate and coefficient of friction.

In this study RSM was the tool used to derive the optimized wear rate and coefficient of friction values. Table 7 depicts the goals, range, optimal values of the various input parameters and output responses ie. wear rate, coefficient of friction. The analysis was made on 31 different input parameter pairs as shown in Table 3. The input parameter pair with highest desirability value is chosen as optimal condition for the output responses. The ramp function graph and bar graph shown in Fig. 11, indicates the desirability of output responses. The ramp function graph presents a clear picture on prediction of response for particular parameters indicated by a dot. The bar graph (Fig. 13) represents the desirability values of each response and the combined desirability of the model. The optimal region had a combined desirability of 0.90054 which is an indication of closeness to the response target

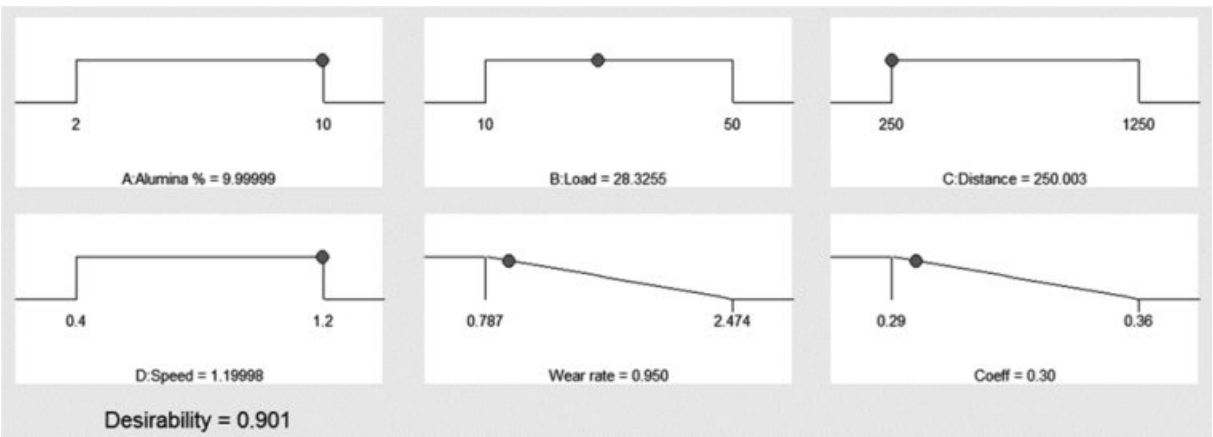

Fig. 12. Ramp function graph of desirability.

Table 7. Parameters range and the responses of desirability.

S.No	Process parameter	Goal	Lower limit	Upper limit	Optimum Value	Importance
1	Reinforcement (%)	In range	2	10	9.99	3
2	Load(N)	In range	10	50	28.325	3
3	Distance(m)	In range	250	1250	250.003	3
4	Speed(m/s)	In range	0.4	2.0	1.999	3
5	Wear rate × 10^{-3} (mm^3/m)	minimise	0.787	2.474	0.950	3
6	Coeff of friction	minimise	0.29	0.36	0.30	3

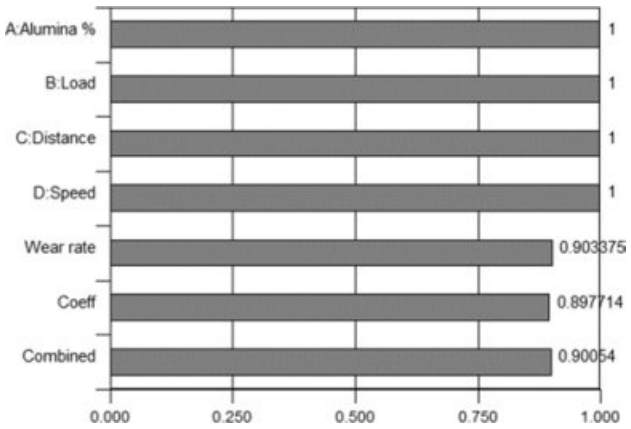

Fig. 13. Bar graph of desirability.

Conclusions

Aluminum alloy reinforced with Al_2O_3 and B_4C of different compositions were prepared by stir casting method. The wear and frictional behaviour of the specimen were studied using pin-on-disc equipment. The major outcome of the current investigations is summarised.

- Al 7075/Al_2O_3/B_4C matrix composite were manufactured successfully with a uniform dispersion of particulates in the matrix which was authenticated by the SEM micro graph and XRD.
- RSM Box Behnken design method was employed to develop the model with 95% confidence level.
- A numerical model was developed to predict the wear rate and coefficient of friction of aluminium hybrid composites incorporating the effects of percentage of Alumina, sliding distance, applied load, and sliding speed.
- The adequacy of the proposed model was checked using ANOVA method. The result indicates that the developed model has good agreement with the experimental results.
- The 3D interaction plot illustrate that the wear rate decreases with increasing of
- Al_2O_3 content and incremented in increasing of load. The wear rate has a negative impact in increase of sliding speed and sliding distance.
- The coefficient of friction exhibited an inversely proportional relationship with the percentage of reinforcement and sliding speed.
- The input parameters were optimised by adopting Desirability based multi response optimization to minimize the wear rate and coefficient of friction.
- The optimum parameters of combination is % of Alumina 9.99, Load 28.32 N, Sliding distance 250 m, Sliding speed 1.99 m/s, for a minimized wear rate of 0.950X 10^{-3} mm^3/m and coefficient of friction 0.30 with a combined desirability of 0.901.

References

1. M.K. Surappa, Sadhana 28[1-2] (2003) 319-334.
2. D.B. Miracle, Compos. Sci. Technol. 65[15-16] (2005) 2526-2540.
3. J. Eliasson and R. Standstorm, Key Engg Materials 104-107 (1995) 3-36.
4. M.O. Bodunrin, K.K. Alaneme, and L.H. Chown, J. of Mater. Res. Technol. 4[4] (2015) 434-445.
5. J. Hashim, L. Looney, and M.S.J. Hashm, J. Mater. Process. Technol. 92-93 (1999) 1-7.
6. A. Baradeswaran and A. Elaya Perumal, Compos.: Part B 56 (2014) 464-471
7. G.B. Veeresh Kumar, C.S.P Rao, N. Selvaraj, and M.S. Bhagyashekar, J. of Miner. & Mater. Char. & Engg 9[1] (2010) 43-55.
8. K. Ravi Kumar, K.M. Mohanasundaram, G. Arumaikkannu, and R. Subramanian, Tribol. - Mater., Surf. & Inter. 6[1] (2012) 15-19.
9. D.S. Prasad and C. Shoba, J. of Mater. Res. and Technol. 3[2] (2014) 172-178.
10. R. Kumar and S. Chauhan, Measurement 65 (2015) 166-180.
11. T. Rajmohan, K. Palanikumar, and S. Ranganathan, Trans. of Nonferr, Metals Soc. of China 23 (2013) 2509-2517.
12. M. Uthayakumar, S. Aravindan, and K. Rajkumar Mater. and Des. 47 (2013) 456-464.
13. K.R. Kumar, K.M. Mohanasundaram, G. Arumaikkannu, and R. Subramanian, Sci. and Engg of Compos. Mater. 19 (2012) 247-253.
14. N. Radhika and R. Raghu, Tribol Letters, 59[2] (2015) 1-9.
15. K. Ravi kumar, K.M. Mohanasundaram, G. Arumaikkannu, and R. Subramanian, Tribol. Trans 55 (2012) 723-729.
16. S. Selvi and E. Rajasekar, J. of Mech. Science and Technol. 29[2] (2015) 785-792.
17. S. Suresh, N. Shenbaga Vinayaga Moorthi, S.C. Vettivel, and N. Selvakumar, Mater. and Design 59 (2014) 383-396.
18. V. Vembu and G .Ganesan, Defence Technol. 11[4] (2015) 390-395.
19. K. Ravi Kuamr and Nishasoms, Arabian J. of Sci. Eng. 44 (2018) 893-909.
20. K. Ravi Kumar and V.S. Sreebalaji, Tribol. 9[3] (2015) 128-136.
21. S.C. Vettivel, N. Selvakumar, R. Narayanasamy, and N. Leema, Mater. and Design, 50 (2013) 977-996.
22. A.K. Lakshminarayanan and V. Balasubramanian, Trans. of Nonferr. Met. Soc. of China 19[1] (2009) 9-18.
23. X. Wang, X. Song, M. Jiang, P. Li, Y. Hu, K. Wang, and H. Liu, Optics & Laser Technol. 44[3] (2012) 656-663.
24. S. Rajakumar, C. Muralidharan, and V. Balasubramanian, Trans. Nonferrous Met. Soc. China 20[10] (2010) 1863-1872.
25. K. Velmanirajan, A. Syed Abu Thaheer, R. Narayanasamy and C. Ahamed Basha, Mater. and Des. 4 (2012) 239-254.
26. N. Radhika, R. Subramanian, S. Venkat Prasat, and B. Anandavel, Indl. Lubr. and Tribol. 64[6] (2012) 359-366.
27. A. Mazahery and M.O. Shabani, Trans. Nonferrous Met. Soc. China 23[7] (2013) 1905-1914.
28. V.C. Uvaraja and N. Natarajan, J. Tribol. 135[2] (2013) 021101.
29. K.M. Shorowordi, A.S.M.A Haseeb, and J.P Celis, Wear 256[11-12] (2004) 1176-1181.
30. M. Abedini, H.M. Ghasemi, and M. Nili Ahmadabadi, Tribol. Transactions 55[5] (2012) 677-684.

31. V.C. Uvaraja and N. Natarajan, J. of Miner. and Mater. Char. and Engg. 11 (2012) 757-768.
32. M. Singh, B.K. Prasad, D.P. Mondal, and A.K. Jha, Tribol. Inter. 34[8] (2001) 557-567.
33. U. Soy, A. Demir, and F. Findik, Indl. Lubr. and Tribol. 63[5] (2011) 387-393.
34. J. Hemanth, Wear 258[11-12] (2005) 1732-1744.
35. T.S. Mahmoud, J. of Mech. Engg Science 222[2] (2008) 257-265.
36. B.M. Girish, B.M. Satish, Sadanand Sarapure, and Basawaraj, Metallur. and Mater. Trans. A 47[6] (2016) 3193-3200.
37. G. Derringer and R. Suich, J. of Qual. Technol. 12[3] (1980) 214-219.
38. K. Kaviyarasan, T. Pridhar, B. Sureshbabu, C. Boopathi, and R. Srinivasan, IOP Conf. Ser.: Mater. Sci. Eng. 402 (2018) 01-07.
39. B. Sureshbabu, G. Chandramohan, C. Boopathi, T. Pridhar, and R. Srinivasan, Int. J. Ceram. Process. Res. 19[1] (2018) 69-74.
40. C. Saravanan, S. Dinesh, P. Sakthivel, V. Vijayan, and B. Suresh Kumar, Mater. Today:. Proc. 21[1] (2020) 744-747.
41. A.E. Pramono, Int. J. Ceram. Process. Res. 20[1] (2019) 01-07.